# Evaluation of mother wavelets on steady-state visually-evoked potentials for triple-command brain-computer interfaces

**Ebru SAYILGAN**[1] , **Yılmaz Kemal YÜCE**[2] , **Yalçın İŞLER**[3,*]
[1]Department of Mechatronics Engineering, İzmir University of Economics, İzmir, Turkey
[2]Department of Computer Engineering, Alanya Alaaddin Keykubat University, Antalya, Turkey
[3]Department of Biomedical Engineering, İzmir Katip Çelebi University, İzmir, Turkey

**Abstract:** Wavelet transform (WT) is an important tool to analyze the time-frequency structure of a signal. The WT relies on a prototype signal that is called the mother wavelet. However, there is no single universal wavelet that fits all signals. Thus, the selection of mother wavelet function might be challenging to represent the signal to achieve the optimum performance. There are some studies to determine the optimal mother wavelet for other biomedical signals; however, there exists no evaluation for steady-state visually-evoked potentials (SSVEP) signals that becomes very popular among signals manipulated for brain-computer interfaces (BCIs) recently. This study aims to explore, if any, the mother wavelet that suits best to represent SSVEP signals for classification purposes in BCIs. In this study, three common wavelet-based features (variance, energy, and entropy) extracted from SSVEP signals for five distinct EEG frequency bands (delta, theta, alpha, beta, and gamma) were classified to determine three different user commands using six fundamental classifier algorithms. The study was repeated for six different commonly-used mother wavelet functions (haar, daubechies, symlet, coiflet, biorthogonal, and reverse biorthogonal). The best discrimination was obtained with an accuracy of 100% and the average of 75.85%. Besides, ensemble learner gives the highest accuracies for half of the trials. Haar wavelet had the best performance in representing SSVEP signals among other all mother wavelets adopted in this study. Concomitantly, all three features of energy, variance, and entropy should be used together since none of these features had superior classifier performance alone.

**Key words:** Steady-state visually-evoked potentials, brain-computer interfaces, wavelet transform, mother wavelet selection, pattern recognition

## 1. Introduction

For many years, researchers have thought that electrophysiological measurements of brain activities can provide a channel to commit messages and/or commands to the outside world and they have conducted many studies for it. During the last 25 years, some productive human-machine interface (HMI) applications have emerged [1]. These applications especially focused on improving communication and control needs of people with some neuromuscular disorders (ALS, brainstem stroke, and spinal cord injury, etc.) [2]. The main objective of these systems is to provide word-processing programs or neuroprosthesis that help partially- or completely-paralyzed patients express their wishes to other people.

In HMI, applications targeting patients with some disabilities, different biomedical signals acquired from the brain (electroencephalography, EEG), cardiac rhythms (electrocardiography, ECG), eye movements

---

*Correspondence: islerya@yahoo.com

(electrooculography, EOG), and various combinations of them have been used since these signals can be acquired relatively easy compared to other types of signals. Nonetheless, some of these patients can maintain their brain activities and produce EEG signals only. In such a context, only EEG signals can be manipulated to enable patients to express themselves. Then, this type of HMI system is called the brain-computer interface (BCI), and it uses brain-related signals [1, 2].

Various methods are available to monitor brain activities including EEG, functional magnetic resonance imaging (fMRI), magnetoencephalography (MEG), positron emission tomography (PET), and optical imaging. However, fMRI, PET, MEG, and optical imaging are not preferred since they are technically difficult and expensive methods compared to EEG methods [3]. Besides, fMRI, PET, and optical imaging methods are less suitable for fast communication as they require a longer time to acquire data. Among these monitoring methods, only EEG-based methods may offer a practical BCI possibility [1–3] since

- it is relatively noninvasive,

- it requires shorter processing time,

- it is relatively available and accessible in most cases, and

- it needs a simpler and cheaper equipment.

Commonly used signals in EEG-based BCIs are slow cortical potentials, *mu* and *beta* rhythms, event-related potentials (ERP), event-related synchronization (ERS), event-related desynchronization (ERD), and visually-evoked potentials (VEP). VEP-based BCI is considered to be a dependent BCI, unlike other systems because VEP depends on stimulating the eye via cranial nerves and extra-ocular muscles. However, this method cannot be applied to a small number of people with severe neuromuscular barriers that may lack the exit channel of extra-ocular muscle control only. Therefore, VEP-based BCI appears to be more suitable than other systems. It has advantages such as high information transfer rate (ITR), simple system structure, shorter user rehabilitation, and shorter time requirement [4].

The VEP is the response of the brain against a visual stimulation. It reflects the visual information processing mechanism in the brain. The steady-state visual evoked potentials (SSVEP) is a response to a modulated visual stimulus that has a frequency higher than 6 Hz [4]. The SSVEP can be recorded on the visual cortex from the scalp with maximum amplitude in the occipital region. In recent studies, SSVEP has received increasing attention as a pivot in the implementation of BCI systems due to its robustness [5].

With the recent advances in system design and signal processing, the performance of SSVEP-based BCIs has improved significantly over the last decade [6, 7]. In general, the structure of an SSVEP-based BCI can be roughly divided into four stages: data acquisition, signal preprocessing, feature extraction, and classification [5]. The first stage is related to acquire the EEG data. The second stage is to apply some well-known processes, i.e. temporal and spatial filtering. The third stage is a methodological attempt to extract meaningful attributes for the characteristics of the selected paradigm. The classifier stage generates a control command using these features extracted from the acquired signal.

There are various methods used in all these stages including the feature extraction stage. However, the discrete wavelet transform (DWT) method, which is known to be effective especially in nonstationary signals during the feature extraction stage, gives relatively better results in EEG-based BCI studies [8–17], compressing the grayscale images [18], filtering angiopraphic images [19], recognizing isolated spoken words

[20, 21], diagnosing epileptic patients [22, 23], determining eye blinks [24], understanding the meditation [25]. When extracting feature(s) with DWT, it is necessary to know which mother wavelet should be used since the performance of the system strictly depends on the representativeness capacity of the extracted features. As a consequence, in the wavelet transform (WT), selecting a suitable mother wavelet is always the first step. Different mother wavelets give different WT coefficients even for the same data segment [26]. Based on the literature search performed within the scope of this study, between 1977 and 2020, the EEG-based studies and efforts that aimed to determine the best mother wavelets were compared in Table 1 to reflect the actual situation in the literature.

**Table 1.** Studies in the literature comparing the EEG signal for different mother wavelets to determine user command(s) where # shows the number of commands.

| Task | Classifiers | Wavelets | # | |
|------|-------------|----------|---|---|
| To discriminate imaginary movements of left-hand, right-hand, and step forward | Bayes Net, SVM, RBF | Sym4 | 3 | [8] |
| To gaze at one stimulus according to single control intention | SVM | Cmor | 1 | [9] |
| To control cursor movements for ALS patients | MLP, PNN (RBF), SVM | Haar | 2 | [10] |
| To control the movement of a small ball on the screen | Fisher classifier | Db40 | 4 | [11] |
| To discriminate imaginary movements of left- and right-hands | Hidden Markov model | Db10 | 2 | [12] |
| To decode finger movements | LDA | Mor | 2 | [13] |
| To discriminate imaginary movements of both fists and both feet | NN | Coif4 | 2 | [14] |
| To classify four different mental tasks | ANN | Coif1 | 4 | [15] |
| To classify five different mental tasks | No classifier | Db | 5 | [16] |
| To determine the visual attention | Statistical evidence | Morlet | 1 | [17] |

In BCI studies, system performance has been generally evaluated using one or two commands in most real-time applications [27]. The reason for this is that when the number of commands increases, the recognition rate of the correct mental state decreases [1, 28]. In other words, parallel to the increase in the number of commands, BCI performance decreases rapidly, which endangers the reliability of the system [27, 29]. However, it is a fact that more commands should be used to provide a more flexible, useful, and efficient system [30]. Thus, in many studies in the literature, they have tested their systems using three commands, both to ensure system reliability and to design a more flexible BCI: The first one is a visual environment navigation application with a BCI based on motor imagery designed by Scherer et al. [31]. In this study, the user can turn left, turn right or move straight in a virtual garden with 3 different commands (left hand, right hand and foot movement). In another study, Benevides et al. [32] aimed to steer a robotic wheelchair using BCI competition III EEG data. The data set, which includes three mental tasks, includes the imagery of the right and left hand movement, and the mental tasks of generating a word starting with the same random letter, respectively. They assigned these tasks as wheelchair right turn, left turn, and straight forward commands, respectively. Some of the studies carried out with the SSVEP signal are: Legény et al. [33], in their game Mind Shooter, provided the movement of the spaceship using 3 different frequencies. In this game, 10 Hz, 12 Hz, and 15 Hz are used, and these frequencies are commanded to move right, move left, and shoot, respectively. In another study of the same

team, [34] directed a virtual butterfly with the frequencies of 12 Hz, 15 Hz, and 20 Hz to move to the right, left, and straight, respectively. In the study by Chung et al. [35], the left-hand movement, right-hand movement, and stop commands of the humanoid robot in a virtual house were provided with frequencies of 12 Hz, 15 Hz, and 20 Hz. In another study, Farell et al. [36], by using the same frequencies as the previous study, triggered an avatar make it raise its left hand, press the button, and lower its left hand again. In addition, Babu et al. [16] determined the PSD features only from the flickering frequencies of 6.67 Hz, 7.50 Hz, 8.57 Hz, 10.00 Hz, and 12.00 Hz. Finally, de Lissa et al. [17] investigated the statistically meaningful differences between gaze and no gaze at the flickering frequency of 30 Hz using Morlet wavelets.

In addition to the DWT-based feature extraction BCI studies, DWT has been accepted as a common denoising method in other BCI studies in the literature [37–41]. To our knowledge, the mother wavelet comparison has been made for SSVEP by Zhang, Li, and Deng only. The best performance achieved by this study has been 95%; however, they compared continuous mother wavelets although the SSVEP had a discrete nature [9]. Moreover, analyses were performed only for a single command in their study. Therefore, one can argue that the mother wavelet selection for SSVEP is still an open question.

In addition, whenever the WT is adopted and implemented in a pattern recognition system, a feature and/or features must first be extracted for it [42]. In many studies, energy and/or entropy and/or variance are calculated from heart rate variability (HRV) [43–46], electrocardiography (ECG) [48], electromyography (EMG) [49, 50], electrooculography (EOG) [51], electroencephalography (EEG) [52, 53], steady-state visually-evoked potentials (SSVEP) [53] signals first. When their mathematical formulas are examined, these features seem to be similar. However, in most of these studies, all these features were used together by neglecting their effectiveness in classification.

In this study, effects of the mother wavelet and different wavelet features including energy, entropy, and variance for SSVEP signals were investigated to determine which combination of the mother wavelet, and feature group has a greater discrimination power on BCI studies classifying three commands at the same time.

## 2. Materials and methods

The methodological approach of this study is summarized in the following block diagram (Figure 1). In accordance, wavelet coefficients were calculated using six different mother wavelet types (haar, daubechies, symlet, coiflet, biorthogonal, reverse biorthogonal) from the EEG data set containing the SSVEP data. The rest of the algorithm was repeated for each of these six different mother wavelet types. First, computed wavelet coefficients were grouped into five different EEG frequency bands (delta, theta, alpha, beta, and gamma). In the next step, the features were generated by calculating the energy, entropy, and variance values from the wavelet coefficients obtained for each frequency band. After this stage, all the features were applied to the input of the classification algorithms, then the features are applied separately. When different subtypes of the six basic classifier algorithms were included, twenty-four different classification procedures were run respectively.

### 2.1. Dataset description and preprocessing

In this study, the dataset (AVI SSVEP Dataset) containing SSVEP signals designed and recorded by Adnan Vilic was used[1]. The data set consists of EEG measurements of the triggered responses of SSVEP signals from 4 healthy individuals while they were looking at the flashing target with three different frequencies. Table

---

[1]Adnan Vilic (2013). AVI steady-state visual evoked potential (SSVEP) signals dataset [online]. Website: https://www.setzner.com/avi-ssvep-dataset [accessed 14.10.2020].
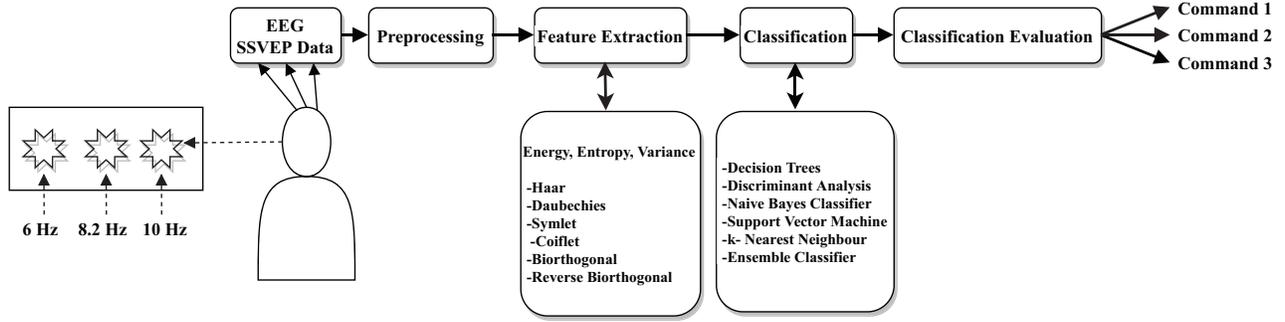
**Figure 1.** Block diagram of the proposed study.

2 presents the physiological knowledge (gender and age) of these participants in the experiment. All EEG data were recorded using three electrodes (Oz, Fpz, and Fz) from the standard international 10–20 system for electrode placement. The sampling frequency of the EEG signal is 512 Hz. The reference electrode was positioned in Fz with the signal electrode in Oz and Fpz in the ground electrode. Besides, the entire data set is freely available and accessible.

**Table 2.** List of participants (male (M), female (F)).

| Participant | 1 | 2 | 3 | 4 |
|---|---|---|---|---|
| Gender | M | M | M | F |
| Age | 32 | 27 | 27 | 31 |

Subjects sat in front of an LCD computer display with a refresh rate of 120 Hz. Contrast and brightness were set to maximum. Besides, the screen resolution was $1680 \times 1050$ pixels. The targets presented to the subjects were arranged to have an area of $2.89cm^2$. An application was developed in Microsoft Silverlight to display the visual stimulus to subjects and was run on a Windows 8-based computer. An analog notch filter was applied to the data obtained at interference frequency (50Hz). The data were saved as both Matlab (MathWorks, Inc., Natick, MA, USA) and text files.

In this experiment, individuals have seated 60 cm away from a monitor staring at a single flashing target whose color changed rapidly from black to white. The test stimulus is a flashing box at 7 different frequencies (6 - 6.5 - 7 - 7.5 - 8.2 - 9.3 - 10 Hz) presented on the monitor. Although the data set included these 7 different frequencies, 3 frequencies (6, 8.2, and 10 Hz) among them with larger differences were selected for this study.

The dataset was acquired through four sessions, i.e. one session for each participant. Each session was conducted with three identical experiments. Each experiment yielded EEG data for seven frequencies with short breaks among them and took 30 s.

## 2.2. Wavelet-based feature extraction

Feature extraction is the process of obtaining the information hiding in EEG signals [54–56]. Time-domain, frequency-domain, and time-frequency features have been used in EEG- and SSVEP-based systems [57]. One of the most popular signal processing methods of these signals is wavelet transform (WT) [22]. There are two major reasons to use WT. First, WT is an effective method yield the signal in the both time and frequency domains. Second, WT is a robust transformation method in nonstationarity signals like all biomedical signals [18, 20].

In this study, as feature vectors, features have been calculated by using the DWT [18]. As the first step of the feature extraction phase, the signal is passed through a series of high-pass filters to analyze the high-frequency changes in the signal, and through a series of low-pass filters to analyze the low-frequency changes. The signal obtained by subsampling the signal at the low-pass filter output is called the approximate coefficients (A), while the one in at the high-pass filter output is called the detail coefficients (D). Figure 2 shows these wavelet coefficients for 9-level decomposition of DWT.
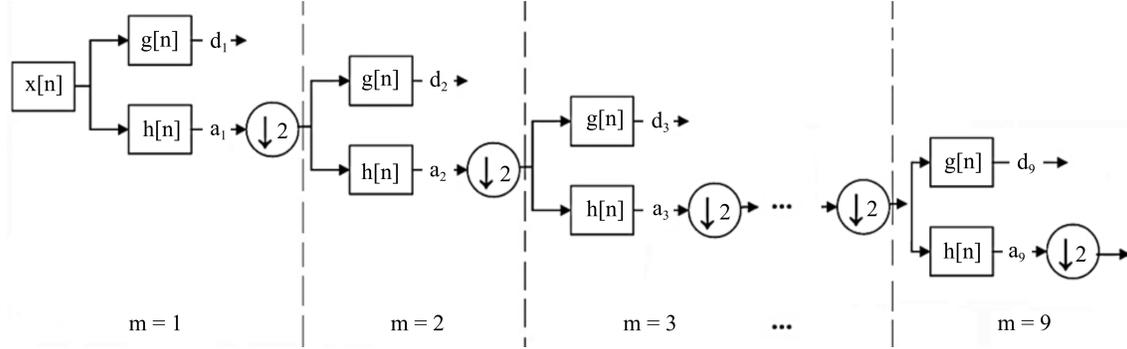


**Figure 2.** 9-level decomposition in the discrete wavelet transform.

Using different DWT functions (haar, daubechies (DB), symlets (SYM), coiflets (COIF), biorthogonal (BIOR), reverse biorthogonal (RBIO)), EEG signals are subdivided into frequency bands. Wavelet families, which are compared in the presented study, where mother wavelet types are used for EEG signals in the literature.Thus, features of energy, entropy, and variance were obtained from A and D coefficients for corresponding EEG bands [22].

The energy of each coefficient was calculated using the following equation:

$$E_j = C_j^2 \tag{1}$$

$C_j$ in the equation expresses each of the wavelet coefficients formed by the wavelet level corresponding to each EEG band [52]. Total energy of an EEG band, $E_f$, was calculated separately for EEG bands:

$$E_f = \sum_{j \in f} E_j \tag{2}$$

Here, $f$ represents the the EEG frequency band [52].

Another feature, entropy ($WS_f$), was calculated as follows:

$$WS_f = -\sum_{j \in f} (p_j log_2(p_j)) \tag{3}$$

Here, the probability of energies of all frequency ($f$) values in the frequency band of interest is calculated as $p_j$ [51] and $p_j$ is the value obtained by dividing the energy of the frequency of interest by the total energy ($\frac{E_j}{E_total}$).

Once the wavelet coefficients are known, the variance of each wavelet level can be calculated as follows:

$$D_f = \sum_{j \in f} (C_j - \overline{C_f})^2 \tag{4}$$

Where $C_j$ is the j-th value of the wavelet coefficient, and $\overline{C_f}$ is the average value of all wavelet coefficients at the EEG frequency band of $f$ [44–46].

These features were applied to the input of classifiers with different combinations: energy features only, entropy features only, variance features only, all these features together.

## 2.3. Classification of signals

To recognize and convert an SSVEP signal to a command, that is to use it as output, classification is performed after the feature extraction stage [3]. For the classification process, there are two substages. First, the classifier parameters are determined by using known data, which is called training. After the training, a decision mechanism algorithm is used to assign the unknown inputs to the appropriate classes [42], which is called testing. In the classification phase, there is no universal classifier to solve all pattern recognition problems. There is no exception for EEG-based BCI systems. Therefore, in this study, feature vectors extracted from the SSVEP signal were tested with twenty-four commonly-used algorithms of the six basic classifiers by applying different algorithm-specific parameters. These classifiers were implemented using the Matlab software (Matlab Inc.): decision trees (*fine, medium, coarse*), discriminant analysis (*linear, quadratic*), naive bayes (*Gaussian, Kernel-based*), support vector machines (*linear, quadratic, cubic, fine Gaussian, medium Gaussian, coarse Gaussian*), k-nearest neighbors (*fine, medium, coarse, cubic, cosine, weighted*), and ensemble classifiers (*boosted, bagged, subspace discriminant, subspace KNN, RUSBoosted trees*).

## 2.4. Evaluating classifier performances

The *k*-fold cross-validation and confusion matrix evaluation criteria were used to evaluate the performance of the classification algorithms used in this study.

### 2.4.1. *k*-fold cross-validation

The feature set consisting of the features extracted from the data sets is divided into train and test sets. Although parameters of a classifier are adjusted using the training set, the classifier performance is tested using the test set. It is necessary to achieve a good generalization performance for a classifier [42]. One of the most commonly used methods for dividing the data set as a train and test sets is the *k*-fold cross-validation method. In this method, the data set is randomly divided into *k* segments. Among these segments, *k*-1 parts are used for the training and the remaining part is used for the testing. This process is repeated until all parts are used for testing separately. The test errors are recorded each time and the average of the errors after the last part is reported. The performance of the classifier algorithm used is evaluated using this validation approach [47]. In this study, the data set is divided into five equal parts (Figure 3).

### 2.4.2. The confusion matrix

The confusion matrix is calculated for evaluating classifier performances. It is generated by comparing the responses of the classification algorithm to the test set with the actual values in the data set. In the case of three-state problems, it is a table consisting of nine different situations only (Table 3) [42]:
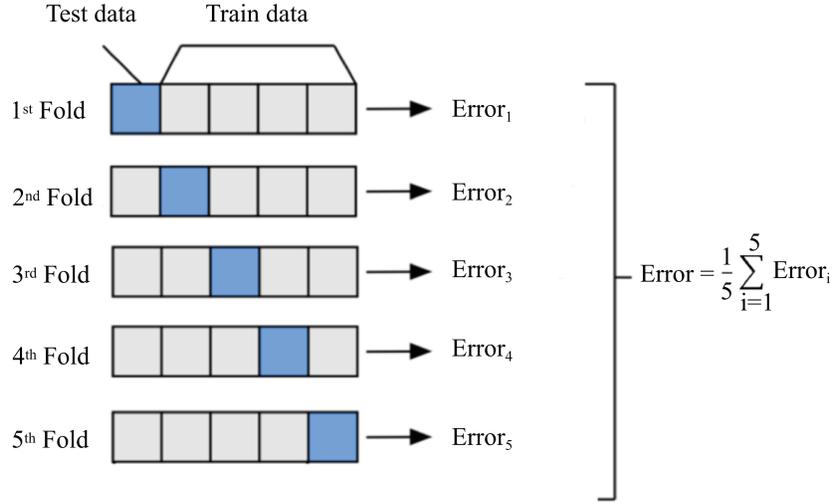
**Figure 3.** *k*-fold cross-validation model used in the classification of this study with k=5.

**Table 3.** $3 \times 3$ confusion matrix for 6 - 8.2 - 10 classes.

|  |  | Predicted class | | |
|---|---|---|---|---|
|  |  | 6 Hz | 8.2 Hz | 10 Hz |
| Actual class | 6 Hz | a | b | c |
|  | 8.2 Hz | d | e | f |
|  | 10 Hz | g | h | i |

Overall accuracy (ACC) value is calculated as classifier performance based on these values [42]:

$$ACC = \frac{a + e + i}{a + b + c + d + e + f + g + h + i} \tag{5}$$

## 2.5. Experimental design

In accordance with the objective of our study, we have designed it in a two-fold manner. First, we measured the accuracy of each (feature, mother wavelet function) pair. In the second part, we combined the set of three features with each mother wavelet function in order to discover which mother wavelet function leads to the best performance.

## 2.6. Implementation details

Three important features (i.e. energy, variance, and entropy) have been extracted for EEG bands (i.e. delta, theta, alpha, beta, and gamma) using six different mother wavelet families (haar, db, sym, coif, bior, rbio). To this purpose, algorithms were implemented using signal processing toolbox and wavelet toolbox in Matlab 2019a (Matlab Inc.). All the classifiers and performance analyses were implemented using the classification learner app tool from Matlab version 2019a (Matlab Inc.).

## 3. Results and discussion

As the results of the first part of the experimental design, the classification accuracies are obtained for each feature (energy, entropy, and variance) extracted using each wavelet family for 4 participants. Mean, minimum, and maximum values of the classification results are presented in Figure 4. Features obtained from the haar wavelet function yielded higher accuracies than those obtained from the other wavelet functions. Haar resulted in the accuracies of 75.85%, 73.08%, and 73.75% for energy, entropy, and variance features, respectively. There are no major differences among the mean values of the 3 features extracted based on the haar wavelet. However, the entropy feature had a noticeable maximum accuracy of 100% compared to the others.
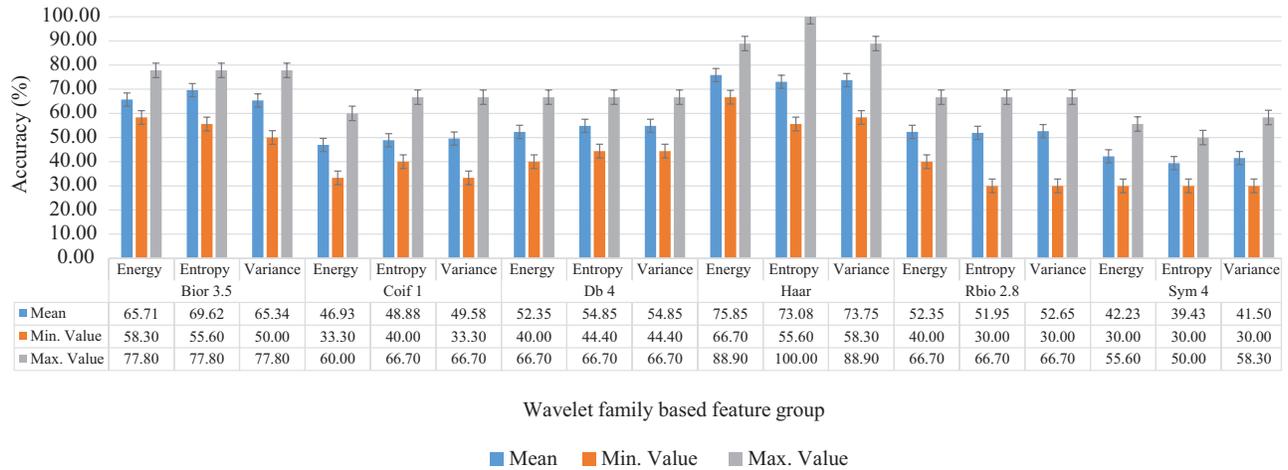


| | Energy | Entropy Bior 3.5 | Variance | Energy | Entropy Coif 1 | Variance | Energy | Entropy Db 4 | Variance | Energy | Entropy Haar | Variance | Energy | Entropy Rbio 2.8 | Variance | Energy | Entropy Sym 4 | Variance |
|---|---|---|---|---|---|---|---|---|---|---|---|---|---|---|---|---|---|---|
| Mean | 65.71 | 69.62 | 65.34 | 46.93 | 48.88 | 49.58 | 52.35 | 54.85 | 54.85 | 75.85 | 73.08 | 73.75 | 52.35 | 51.95 | 52.65 | 42.23 | 39.43 | 41.50 |
| Min. Value | 58.30 | 55.60 | 50.00 | 33.30 | 40.00 | 33.30 | 40.00 | 44.40 | 44.40 | 66.70 | 55.60 | 58.30 | 40.00 | 30.00 | 30.00 | 30.00 | 30.00 | 30.00 |
| Max. Value | 77.80 | 77.80 | 77.80 | 60.00 | 66.70 | 66.70 | 66.70 | 66.70 | 66.70 | 88.90 | 100.00 | 88.90 | 66.70 | 66.70 | 66.70 | 55.60 | 50.00 | 58.30 |

Wavelet family based feature group

■ Mean   ■ Min. Value   ■ Max. Value

**Figure 4.** Classification performance of energy, entropy, and variance as separate features.

In Table 4, classifier performances of each participant using energy, entropy, and variance features are presented seperately. The highest accuracies were given for each mother wavelet and feature sets. The classifier algorithms, which gave the most successful performance, were given between prantheses just below the accuracies. The average classifier accuracies were also given in the last column of Table 4. Among these algorithms that gave the highest accuracies, the ensemble learner algorithm gave the highest accuracies 43 times.

**Table 4.** Classification performances when energy, entropy, and variance are used as seperate feature sets.

| Mother wavelet | Feature group | Accuracies (%) | | | | |
|---|---|---|---|---|---|---|
| | | Subject 1 | Subject 2 | Subject 3 | Subject 4 | Mean |
| Bior3.5 | Energy | 58.30 | 60.00 | 66.70 | **77.80** | 65.70 |
| | | (Ensemble) | (SVM) | (Ensemble) | (Ensemble) | |
| | | | (KNN) | | | |
| | | | (Ensemble) | | | |
| | Entropy | **75.00** | **70.00** | 55.60 | **77.80** | 69.60 |
| | | (LDA) | (SVM) | (Ensemble) | (Ensemble) | |
| | | | (KNN) | | | |
| | | | (Ensemble) | | | |
| | Variance | 66.70 | 50.00 | 66.70 | **77.80** | 65.30 |
| | | (LDA) | (Naive Bayes) | (Ensemble) | (Ensemble) | |
| | | | (KNN) | | | |
| | | | (Ensemble) | | | |
| Coif1 | Energy | 50.00 | 60.00 | 44.40 | 33.30 | 46.93 |
| | | (SVM) | (LDA) | (LDA) | (Naive Bayes) | |
| | | (KNN) | | | | |

**Table 4.** (Continued)

| | | | | | |
|---|---|---|---|---|---|
| | | (Ensemble) | | | | |
| | Entropy | 66.70 (Ensemble) | 40.00 (LDA) (Naive Bayes) | 44.40 (LDA) | 44.40 (Naive Bayes) | 48.88 |
| | Variance | 58.30 (SVM) | 40.00 (LDA) (Ensemble) | 66.70 (LDA) | 33.30 (KNN) (Ensemble) | 49.58 |
| Db4 | Energy | 58.30 (Ensemble) | 40.00 (SVM) (Ensemble) | 44.40 (Ensemble) | 66.70 (Naive Bayes) | 52.35 |
| | Entropy | 58.30 (SVM) (Ensemble) | 50.00 (Ensemble) | 44.40 (SVM) (Naive Bayes) | 66.70 (Ensemble) | 54.85 |
| | Variance | 58.30 (Ensemble) | 50.00 (Ensemble) | 44.40 (Ensemble) (Naive Bayes) | 66.70 (Naive Bayes) | 54.85 |
| **Haar** | **Energy** | 66.70 (Decision tree) | **70.00** (Ensemble) | 88.90 (LDA) | **77.80** (Ensemble) | **75.85** |
| | Entropy | 66.70 (Decision tree) | **70.00** (Ensemble) | **100.0** (LDA) | 55.60 (Ensemble) | 73.08 |
| | ariance | 58.30 (Naive bayes) | **70.00** (Ensemble) | 88.90 (LDA) | **77.80** (Ensemble) | 73.75 |
| Rbio2.8 | Energy | 58.30 (SVM) | 40.00 (Ensemble) | 44.40 (LDA) (Ensemble) | 66.70 (Ensemble) | 52.35 |
| | Entropy | 66.70 (LDA) | 30.00 (Naive Bayes) | 44.40 (Ensemble) | 66.70 (LDA) | 51.95 |
| | Variance | 58.30 (SVM) | 30.00 (Ensemble) | 55.60 (Ensemble) | 66.70 (Ensemble) | 52.65 |
| Sym4 | Energy | 50.00 (SVM) (KNN) (Ensemble) | 30.00 (Ensemble) | 33.30 (LDA) (SVM) | 55.60 (Ensemble) | 42.23 |
| | Entropy | 50.00 (SVM) (KNN) (Ensemble) | 30.00 (LDA) | 33.30 (SVM) | 44.40 (Ensemble) | 39.43 |
| | Variance | 58.30 (SVM) (Ensemble) | 30.00 (LDA) (Ensemble) | 33.30 (SVM) | 44.40 (Ensemble) | 41.50 |

In the second part of our experimental design, the extracted features were grouped as a single feature set. With reference to results obtained (Figure 5), it is obvious that the most successful wavelet family was the haar wavelet function. The performance ranking in other wavelet families is the same with the first part. The accuracy values are as follows: 75.85% with haar mother wavelet, 67.53% with bior3.5 mother wavelet, 60.85% with db4 mother wavelet, 56.25% with coif1 mother wavelet, 52.35% with rbio2.8 mother wavelet and 44.73% with sym4 mother wavelet. Grouping the features had an impact, both positive and negative, on classifier performances. The mean accuracies of Coif1, Db4, and Sym4 had a significant increase of 6.7%, 6.0%, and 2.5%, respectively; whereas, Bior3.5's mean accuracy decreased by 1.9%.
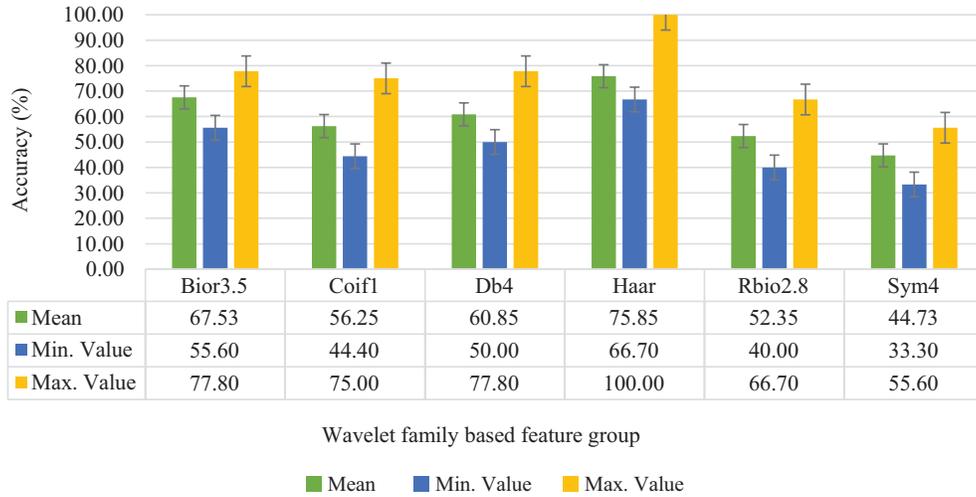
| | Bior3.5 | Coif1 | Db4 | Haar | Rbio2.8 | Sym4 |
|---|---|---|---|---|---|---|
| ■ Mean | 67.53 | 56.25 | 60.85 | 75.85 | 52.35 | 44.73 |
| ■ Min. Value | 55.60 | 44.40 | 50.00 | 66.70 | 40.00 | 33.30 |
| ■ Max. Value | 77.80 | 75.00 | 77.80 | 100.00 | 66.70 | 55.60 |

Wavelet family based feature group

■ Mean   ■ Min. Value   ■ Max. Value

**Figure 5.** Classification performance of energy, entropy, and variance as a unique feature set.

In Table 5, classifier performances of each participant using energy, entropy, and variance features together are presented. The highest accuracies were given for each mother wavelets. The classifier algorithms, which gave the most successful performance, were given between prantheses just below the accuracies. The average classifier accuracies were also given in the last column of Table 5. Among these algorithms that gave the highest accuracies, the ensemble learner algorithm gave the highest accuracies 12 times.

**Table 5.** Classification performances when energy, entropy, and variance are used as a single feature set.

| Mother wavelet | Accuracies (%) | | | | |
|---|---|---|---|---|---|
| | Subject 1 | Subject 2 | Subject 3 | Subject 4 | Mean |
| Bior3.5 | 66.70 (LDA) | **70.00** (KNN) | 55.60 (Ensemble) | **77.80** (Ensemble) | 67.53 |
| Coif1 | **75.00** (LDA) (Ensemble) | 50.00 (Naive Bayes) (Ensemble) | 55.60 (LDA) (Ensemble) | 44.40 (Naive Bayes) | 56.25 |
| Db4 | 50.00 (SVM) (KNN) | 60.00 (KNN) | 55.60 (Naive Bayes) | **77.80** (LDA) | 60.85 |
| **Haar** | 66.70 (LDA) | **70.00** (Ensemble) | **100.0** (LDA) | 66.77 (Ensemble) | **75.85** |
| Rbio2.8 | 58.30 (SVM) | 40.00 (LDA) (Naive Bayes) (Ensemble) | 66.70 (Ensemble) | 44.40 (Ensemble) | 52.35 |
| Sym4 | 50.00 (SVM) (KNN) (Ensemble) | 40.00 (LDA) | 33.30 (SVM) | 55.60 (Ensemble) | 44.73 |

From the literature, Mistry et al. [41] achieved a mean accuracy of 79.4% to discriminate four user commands from SSVEP signals. Mishchenko et al. [39] achieved the mean accuracy of 77% using SVM and 75% using LDA classifiers to discriminate three user commands from EEG signals. Shao et al. [37] achieved the maximum accuracy of 89.92% using canonical correlation analysis (CCA) to classify four user commands from SSVEP signals after wavelet-based denoising. Similarly, Erkan and Akbaba [38] found the highest accuracy of 100% using CCA and minimum energy combination (MEC) to discriminate four user commands from EEG signals after wavelet-based denoising. Finally, in a very recent study, Heidari et al. [2] investigated four different algorithms to obtain three distinct user commands from SSVEP signals. They achieved the maximum accuracy of 91.39% using the k-NN classifier, 89.34% using the SVM classifier, 72.52% using the Bayes classifier, and 59.55% using the MLP classifier. These results are achieved by using all time-domain, frequency-domain, and nonlinear features together and/or applying feature selection algorithms. In this study, we used only common features extracted from the wavelet transform. By regarding this fact, the achieved results seem satisfactory for SSVEP-based BCI designs.

On the other hand, the database consisting of SSVEP data obtained from only four subjects, including 3 men and 1 woman, is the weakness of this study. The findings obtained in our study, which is a preliminary research in character, need to be supported by another study with a larger data set.

Our study might lead a path for those future studies bringing dwt and machine learning methods to analyze SSVEP signals for use in BCIs. In this respect, other power spectral density estimation methods including Gabor transform, Wigner–Wille distributions, Lomb–Scargle periodogram, autoregressive modeling, and moving average modeling, and especially Fourier transform should be investigated. In such a follow-up study, it may be possible to obtain which frequency conversion method and parameter combinations are most convenient in SSVEP-based BCI studies.

## 4. Conclusion

In this study, the type of mother wavelet that presents optimal performance for classification of SSVEP signals was explored with respect to accuracy measure. The adopted open access dataset includes SSVEP signals that were obtained by showing pictures to four subjects (1 female, 3 males). It is aimed to estimate the pictures shown to the subjects in seven different frequencies; however, with three selected stimulation frequencies were adopted within the scope of this study. Using the dataset, energy, variance, and entropy features were calculated by means of the DWT for five different EEG bands. For this purpose, six commonly used wavelet functions (haar, daubechies, symlet, coiflet, biorthogonal, reverse biorthogonal) that are known to have high representation performances in EEG signals have been selected to extract features. Each of these three features (i.e. energy, entropy, and variance) extracted from aforementioned wavelet functions have been used as separate single feature vector. The fourth feature vector was formed by using all three features. As a result of the classification processes performed separately for each subject, when the performances of both feature groups were examined, the most successful wavelet function was found to be the haar wavelet. When the average accuracy values of the feature groups are examined, the results of the feature vector with three features together gave higher results for all wavelet functions than the other feature groups. Although there is no dominant one among energy, entropy, and variance features, the highest result was achieved by the entropy feature in Subject 3 (Table 4) with 100%. When performances of machine learning algorithms have been examined and compared, it is apparent that the ensemble learning algorithm has the highest classification performance.

---

[2]Heidari H, Einalou Z, Dadgostar M, Hosseinzadeh H. A comparison of the analysis of methods for feature extraction and classification by wavelet transform in SSVEP BCIs. Brain Informatics 2020; Under review.

The major aim of this study was to discover type of mother wavelet that could be effective in extraction of features within SSVEP signals to be used in BCI applications. Consequently, classification was executed based on only those features which can be acquired through wavelet transformation. In order to achieve higher accuracy results, use of time-domain features together with haar wavelet-based features is suggested.

Concomitantly, it was aimed to find out if there exists a wavelet feature with high classification performance. Results indicate that none of these features alone has achieved high accuracy with all subjects. The feature vector having all three features together, however, has reached highest classification accuracies in every case, for which single-featured feature vectors have all lower accuracies. Ergo, in BCI studies, forming the feature vector with three wavelet-based features adopted in this study; i.e. energy, entropy, and variance, and executing one of the feature selection algorithms, where and when necessary, might positively impact and improve classification accuracy. In conclusion, if the wavelet transform is used in a SSVEP-based BCI study, the use of energy, entropy, and variance features calculated from haar wavelet should be preferred.

## Acknowledgment

## Conflict of Interest
The authors declare that there is no conflict of interest.

## References

[1] Wolpaw JR, Birbaumer N, McFarland DC, Pfurtscheller G, Vaughan TM. Brain–computer interfaces for communication and control. Clinical Neurophysiology 2002; 113 (6): 767-791. doi: 10.1016/s1388-2457(02)00057-3

[2] McFarland DJ, Wolpaw JR. Brain-computer interfaces for communication and control. Communications of the Association for Computing Machinery (ACM) 2011; 54 (5): 60-66. doi: 10.1145/1941487.1941506

[3] Vidal JJ. Real-time detection of brain events in EEG. Proceedings of the IEEE 1977; 65: 633-641. doi: 10.1109/PROC.1977.10542

[4] Wang YJ, Wang RP, Gao XR, Hong B, Gao SK. A practical VEP-based brain-computer interface. IEEE Transactions on Neural Systems and Rehabilitation Engineering 2006; 14: 234-239. doi: 10.1109/TNSRE.2006.875576

[5] Wang Y, Gao X, Hong B, Jia C, Gao S. Brain-computer interfaces based on visual evoked potentials. IEEE Engineering in Medicine and Biology Magazine 2008; 27 (5): 64-71. doi: 10.1109/MEMB.2008.923958

[6] Chen X, Wang Y, Nakanishi M, Gao X, Jung T et al. High-speed spelling with a noninvasive brain-computer interface. Proceedings of the National Academy of Sciences 2015; 112 (44): E6058-67. doi: 10.1073/pnas.1508080112

[7] Lotte F, Congedo M, Lecuyer A, Lamarche F, Arnaldi B. A review of classification algorithms for EEG-based brain–computer interfaces. Journal of Neural Engineering 2007; 4 (2): R1-R13. doi: 10.1088/1741-2560/4/2/R01.

[8] Mohamed EA, Yusoff MZK, Selman NK, Malik AS. Enhancing EEG signals in brain computer interface using wavelet transform. International Journal of Information and Electronics Engineering 2014; 4 (3): 234-238. doi: 10.7763/IJIEE.2014.V4.440

[9] Zhang Z, Li X, Deng Z. A CWT-based SSVEP classification method for brain-computer interface system. International Conference on Intelligent Control and Information Processing 2010; 43-48. doi: 10.1109/ICICIP.2010.5564336

[10] Kousarrizi MRN, Ghanbari AA, Teshnehlab M, Shorehdeli MA, Gharaviri A. Feature extraction and classification of EEG signals using wavelet transform, SVM and artificial neural networks for brain computer interfaces. 2009 International Joint Conference on Bioinformatics, Systems Biology and Intelligent Computing 2009; 352-355. doi: 10.1109/IJCBS.2009.100

[11] Bian Y, Li H, Zhao L, Yang G, Geng L. Research on steady state visual evoked potentials based on wavelet packet technology for brain-computer interface. Procedia Engineering 2011; 15: 2629-2633. doi: 10.1016/j.proeng.2011.08.494

[12] Mumtaz M, Afzal M, Mushtaq A. Sensorimotor cortex EEG signal classification using hidden markov models and wavelet decomposition. In: 2018 IEEE International Symposium on Signal Processing and Information Technology (ISSPIT), Louisville, KY, USA 2018; 375-381. doi: 10.1109/ISSPIT.2018.8642672

[13] Salyers JB, Dong Y, Gai Y. Continuous wavelet transform for decoding finger movements from single-channel EEG. IEEE Transactions on Biomedical Engineering 2019; 66 (6): 1588-1597. doi: 10.1109/TBME.2018.2876068.

[14] Alomari MH, Awada EA, Samaha A, Alkamha K. Wavelet-based feature extraction for the analysis of EEG signals associated with imagined fists and feet movements. Computer and Information Science 2014; 7 (2): 17-27. doi:10.5539/cis.v7n2p17

[15] Uyulan C, Erguzel TT. Comparison of wavelet families for mental task classification. The Journal of Neurobehavioral Sciences 2016; 3 (2): 59-64. doi: 10.5455/JNBS.1454666348.

[16] Babu B, Chandrasekaran R, Joseph JE, Rahul TS, Thamizhvani TR et al. A study on wavelet analysis of SSVEP signals. International Journal of Engineering & Technology 2018; 7 (2.25): 10-13. doi: 10.14419/ijet.v7i2.25.12354

[17] de Lissa P, Caldara R, Nicholls V, Miellet S. In pursuit of visual attention: SSVEP frequency-tagging moving targets. PLoS ONE 2020; 15 (8): e0236967. doi:10.1371/journal.pone.0236967.

[18] Varuneshkumar M, Anil K, Jaiswal AK. Performance comparison of daubechies, biorthogonal and haar transform for grayscale image compression. International Journal of Computer Applications 2015; 126 (9): 40-42. doi: 10.5120/ijca2015906190

[19] Dogra A, Goyal B, Agrawal S. Performance comparison of different wavelet families based on bone vessel fusion. Asian Journal of Pharmaceutics 2016; 10 (4): S791-S795. doi: 10.22377/ajp.v10i04.989.

[20] Sonia S, David PS, Poulose J. A comparative study of wavelet based feature extraction techniques in recognizing isolated spoken words. International Journal of Signal Processing Systems 2013; 1 (1): 49-53. doi: 10.12720/ijsps.1.1.49-53

[21] Sunny S, Peter D, Jacob KP. Performance analysis of different wavelet families in recognizing speech. International Journal of Engineering Trends and Technology 2013; 4 (4): 512-517.

[22] Gandhi T, Panigrahi KB, Anand S. A comparative study of wavelet families for EEG signal classification. Neurocomputing 2011; 74 (17): 3051-3057. doi: 10.1016/j.neucom.2011.04.029.

[23] Wijayanto I, Rizal A, Hadiyoso S. Multilevel wavelet packet entropy and support vector machine for epileptic EEG classification. In: 2018 4th International Conference on Science and Technology 2018; 1-6. doi: 10.1109/ICSTC.2018.8528634

[24] Poorna SS, Raghav R, Nandan A, Nair GJ. EEG based control - a study using wavelet features. 2018 International Conference on Advances in Computing, Communications and Informatics 2018; 550-553.

[25] Gupta N, Sood N, Saini I. Statistical feature based comparison of EEG in meditation for various wavelet. In: 2018 First International Conference on Secure Cyber Computing and Communication 2018; 73-77. doi: 10.1109/ICSCCC.2018.8703266

[26] Garg, G. A signal invariant wavelet function selection algorithm. Medical & Biological Engineering & Computing 2016; 54: 629-642. doi: 10.1007/s11517-015-1354-z.

[27] Lotte F, Faller J, Guger C, Renard Y, Pfurtscheller G, et al. Combining BCI with virtual reality: towards new applications and improved BCI. In: Allison BZ, Dunne S, Leeb R, Millan JDR, Nijholt A (editors). Towards Practical Brain-Computer Interfaces. Heildelberg, Berlin, Germany: Springer-Verlag, 2013. pp. 197-220. doi: 10.1007/978-3-642-29746-5_10

[28] Obermaier B, Neuper C, Guger C, Pfurtscheller G. Information transfer rate in a five-classes brain-computer interface. IEEE Transactions on Neural Systems and Rehabilitation Engineering 2000; 9 (3): 283-288. doi: 10.1109/7333.948456

[29] Sharma K, Kar S. Extracting multiple commands from a single SSVEP flicker using eye-accommodation. Biocybernetics and Biomedical Engineering 2019; 39(3): 914-922. doi: 10.1016/j.bbe.2019.08.002.

[30] Lotte F, van Langhenhove A, Lamarche F, Ernest T, Renard Y et al. Exploring large virtual environments by thoughts using a brain-computer interface based on motor imagery and high-level commands. Teleoperators and Virtual Environments, Massachusetts Institute of Technology Press 2010; 19(1): 54-70.

[31] Scherer R, Lee F, Schlogl A, Leeb R, Bischof H et al. Toward self-paced brain–computer communication: navigation through virtual worlds. IEEE Transactions on Biomedical Engineering 2008; 55 (2): 675-682. doi: 10.1109/TBME.2007.903709.

[32] Benevides A B, Sarcinelli-Filho M, Bastos Filho T F. Design of a general brain-computer interface. SBA Controle & Automacao 2011; 22 (6): 638-646. doi: 10.1590/S0103-17592011000600009

[33] Legeny J, Viciana-Abad R, Lecuyer A. Toward contextual SSVEP-based BCI controller: smart activation of stimuli and control weighting. IEEE Transactions on Computational Intelligence and AI in Games 2013; 5 (2): 111-116. doi: 10.1109/TCIAIG.2013.2252348

[34] Legeny J, Viciana-Abad R, Lecuyer A. Navigating in virtual worlds using a self-paced SSVEP-based brain–computer interface with integrated stimulation and real-time feedback. Presence: Teleoperators and Virtual Environments 2011; 20 (6): 529-544.

[35] Chung M, Cheung W, Scherer R, Rao R. A hierarchical architecture for adaptive brain-computer interfacing. In: Proceedings of the Twenty-Second International Joint Conference on Artificial Intelligence 2011; 2: 1647-1652, Barcelona, Catalonia, Spain, July 16-22, 2011.

[36] Faller J, Muller-Putz G, Schmalstieg D, Pfurtscheller G. An application framework for controlling an avatar in a desktop-based virtual environment via a software SSVEP brain–computer interface. Presence Teleoperators & Virtual Environments 2010; 19 (1): 25-34. doi: 10.1162/pres.19.1.25.

[37] Shao L, Zhang L, Nasreddine Belkacem A, Zhang Y, Chen X et al. EEG-controlled wall-crawling cleaning robot using SSVEP-based brain-computer interface. Journal of Healthcare Engineering 2020; 6968713: 1-11. doi: 10.1155/2020/6968713

[38] Erkan E, Akbaba M. A study on performance increasing in SSVEP based BCI application. Engineering Science and Technology 2018; 21 (3): 421-427. doi: 10.1016/j.jestch.2018.04.002.

[39] Mishchenko Y, Kaya M, Ozbay E, Yanar H. Developing a three- to six-state EEG-based brain–computer interface for a virtual robotic manipulator control. IEEE Transactions on Biomedical Engineering 2019; 66 (4): 977-987. doi: 10.1109/TBME.2018.2865941

[40] Ortner R, Guger C, Prueckl R, Grunbacher E, Edlinger G. SSVEP based brain-computer interface for robot control. Lecture Notes in Computer Science 2010; 6180: 85-90. doi: 10.1007/978-3-642-14100-3_14.

[41] Mistry KS, Pelayo P, Anil DG, George K. An SSVEP based brain computer interface system to control electric wheelchairs. 2018 IEEE International Instrumentation and Measurement Technology Conference (I2MTC), Houston, TX, 2018, 1-6.

[42] Duda RO, Hart PE, Stork DG. Pattern Classification. 2nd ed. New York, NY, USA: Wiley-Interscience, 2000.

[43] Isler Y, Kuntalp M. Combining classical HRV indices with wavelet entropy measures improves to performance in diagnosing congestive heart failure. Computers in Biology and Medicine 2007; 37 (10): 1502-1510. doi: 10.1016/j.compbiomed.2007.01.012

[44] Isler Y, Narin A, Ozer M, Perc M. Multi-stage classification of congestive heart failure based on short-term heart rate variability. Chaos, Solitons & Fractals 2019; 118: 145-151. doi: 10.1016/j.chaos.2018.11.020.

[45] Narin A, Isler Y, Ozer M, Perc M. Early prediction of paroxysmal atrial fibrillation based on short-term heart rate variability. Physica A: Statistical Mechanics and its Applications 2018; 509: 56-65. doi: 10.1016/j.physa.2018.06.022

[46] Isler Y. Discrimination of systolic and diastolic dysfunctions using multi-layer perceptron in heart rate variability analysis. Computers in Biology and Medicine 2016; 76: 113-119. doi: 10.1016/j.compbiomed.2016.06.029.

[47] Isler Y, Narin A, Ozer M. Comparison of the effects of cross-validation methods on determining performances of classifiers used in diagnosing congestive heart failure. Measurement Science Review 2015; 15 (4): 196-201. doi: 10.1515/msr-2015-0027

[48] Khushaba RN, Kodagoda S, Lal S, Dissanayake G. Driver drowsiness classification using fuzzy wavelet-packet-based feature-extraction algorithm. IEEE Transactions on Biomedical Engineering; 58 (1): 121-131. doi: 10.1109/TBME.2010.2077291

[49] Hu X, Wang Z, Ren X. Classification of surface EMG signal using relative wavelet packet energy. Computer Methods and Programs in Biomedicine 2005; 79 (3): 189-195. doi: 10.1016/j.cmpb.2005.04.001.

[50] Wang G, Wang Z, Chen W, Zhuang J. Classification of surface EMG signals using optimal wavelet packet method based on Davies-Bouldin criterion. Medical and Biological Engineering and Computing 2006; 44 (10): 865-872. doi: 10.1007/s11517-006-0100-y

[51] Lv Z, Wu X, Li M, Zhang D. A novel eye movement detection algorithm for EOG driven human computer interface. Pattern Recognition Letters 2010; 31 (9): 1041-1047. doi: 10.1016/j.patrec.2009.12.017

[52] Rosso OA, Blanco S, Yordanova J, Kolev V, Figliola A et al. Wavelet entropy: a new tool for analysis of short duration brain electrical signals. Journal of Neuroscience Methods 2001; 105: 65-75. doi: 10.1016/s0165-0270(00)00356-3

[53] Zhang Y, Xu P, Cheng K, Yao D. Multivariate synchronization index for frequency recognition of SSVEP-based brain–computer interface. Journal of Neuroscience Methods 2014; 221: 32-40. doi: 10.1016/j.jneumeth.2013.07.018

[54] Sayilgan E, Yuce YK, Isler Y. Prediction of evoking frequency from steady-state visual evoked frequency. Natural and Engineering Sciences 2019; 4 (3): 91-99.

[55] Sayilgan E, Yuce YK, Isler Y. Determining gaze information from steady-state visually-evoked potentials. Karaelmas Science and Engineering Journal 2020; 10 (2): 151-157. doi: 10.7212/zkufbd.v10i2.1588.

[56] Sayilgan E, Yuce YK, Isler Y. Estimation of three distinct commands using Fourier Transform of steady-state visual-evoked potentials. Düzce Üniversitesi Bilim ve Teknoloji Dergisi 2020; 8 (4): 2337-2343. doi: 10.29130/dubited.716386

[57] Shiliang SJZ. A review of adaptive feature extraction and classification methods for EEG-based brain-computer interfaces. In: 2014 International Joint Conference on Neural Networks 2014; 1746-1753. doi: 10.1109/IJCNN.2014.6889525